Analyst

ROYAL SOCIETY OF CHEMISTRY

PAPER

View Article Online
View Journal | View Issue

Cite this: *Analyst*, 2021, **146**, 2203

A label-free immunosensor for the detection of a new lung cancer biomarker, GM2 activator protein, using a phosphomolybdic acid/polyethyleneimine coated gold nanoparticle composite†

Kulrisa Kuntamung,[a,b] Padchanee Sangthong,[a,c] Jaroon Jakmunee[a,c,d,e] and Kontad Ounnunkad *[a,c,d,e]

In this work, we report, for the first time, the construction of a label-free electrochemical immunosensor for highly sensitive detection of a new lung cancer biomarker, GM2 activator protein (GM2AP). A polyethyleneimine-coated gold nanoparticle (PEI-AuNP) and phosphomolybdic acid (PMA) modified electrode is developed as a novel redox platform for GM2AP detection. A PEI-AuNP film-modified screen-printed carbon electrode, as a signal amplifier support, was successfully fabricated for the adsorption of PMA redox molecules and is used for signal amplification. Under the optimized conditions, GM2AP detection is based on a decrease in the current response of PMA redox probes proportionally relative to an amount of the immunocomplex. Our sensor exhibits two linear ranges of 0.005–25 and 25–400 ng mL^{-1} with a limit of detection (LOD) of 0.51 pg mL^{-1}. The immunosensor is successfully applied for the determination of GM2AP in both human urine and serum samples. The proposed sensor offers the advantages of simple fabrication, low cost, rapid analysis, satisfactory stability, high selectivity and sensitivity, and good reproducibility. The LOD of the biosensor is approximately 2863 and 1804 fold lower than the clinically relevant levels in human urine and serum, respectively. Our strategy can be used as an alternative non-invasive clinical analysis method for lung cancer screening.

Received 30th October 2020,
Accepted 26th January 2021

DOI: 10.1039/d0an02149k

rsc.li/analyst

Introduction

Lung cancer is the most frequent type of cancer and continues to be an important public health issue, which impacts communities worldwide, causing approximately 1.5 million deaths every year.[1–3] The most important risk factor for lung cancer is cigarette smoking; however, numerous studies have demonstrated that air pollution, especially by fine particulate matter (PM2.5), and genetic factors also contribute to the development of lung cancer.[4,5] Lung cancer mortality may reduce if the sensitivity and rapidity of cancer detection is improved. The most common tools used in the diagnosis of lung cancer include chest X-ray, computed tomography, magnetic resonance imaging, and biopsy; however, these diagnostic tools are of high cost and time consuming. Moreover, some diagnostic tools such as biopsy cause pain and complications to patients. To date, biosensors, particularly the electrochemical immunosensors, are regarded as powerful tools for the detection of many cancer biomarkers due to many advantages such as rapid assay speed, low cost and easy-to-operate instrumentation, and high detection sensitivity.[1,6]

Recently, GM2 activator protein (GM2AP) has become a promising new urinary biomarker for the diagnosis of lung cancer, which is the second leading cause of cancer-related deaths. The expression levels of GM2AP in urine and serum samples from normal healthy controls are 0.18 and 0.18 ng mL^{-1}, respectively.[7] GM2AP is found to be overexpressed in the urine and blood of lung cancer patients, which can be determined with convenient and non-invasive sampling.[7,8] The GM2AP levels in lung cancer patients show an 8.11 fold increase in urine and a 5.41 fold increase in serum compared

[a]*Department of Chemistry, Faculty of Science, Chiang Mai University, Chiang Mai 50200, Thailand. E-mail: suriyacmu@yahoo.com, kontad.ounnunkad@cmu.ac.th*
[b]*The Graduate School, Chiang Mai University, Chiang Mai 50200, Thailand*
[c]*Center of Excellence for Innovation in Chemistry, Faculty of Science, Chiang Mai University, Chiang Mai, 50200, Thailand*
[d]*Research Center on Chemistry for Development of Health Promoting Products from Northern Resources, Chiang Mai University, Chiang Mai, 50200, Thailand*
[e]*Center of Excellence in Materials Science and Technology, Chiang Mai University, Chiang Mai 50200, Thailand*

†Electronic supplementary information (ESI) available. See DOI: 10.1039/d0an02149k

with the healthy group,[7] which can be effectively used for the diagnosis of the disease. According to previous reports, GM2AP is detected using conventional methods such as enzyme-linked immunosorbent assay and western blotting.[7] These methods require a complicated process for sample preparation and many chemicals. They also are time-consuming procedures and have high operating cost. To overcome these drawbacks, electrochemical immunosensors have been proposed as promising devices for rapid, reliable and simple protein biomarker detection.[9] Particularly, label-free electrochemical immunosensors can be used to detect different biological molecules due to their simple handling, low cost, and measurement that does not involve a complicated labelling process.[10,11] Despite their numerous advantages, the development of label-free immunosensors by improving the performances with regard to simplicity, rapid response, sensitivity, detection limit, specificity, and stability still remains a crucial challenge. The use of new materials in the development of novel immunosensing platforms is one of the best ways to enhance such properties, especially sensitivity and specificity.[12]

Gold nanoparticles (AuNPs) have been widely used as signal amplifiers due to their good electrical conductivity, high surface energy, strong adsorption ability, and biocompatibility.[13–16] In previous studies, poly(ethyleneimine)-coated-AuNPs (PEI-AuNPs) were employed as labelling tags in electrochemical sensors for multiplex immunoassay of four tumor biomarkers.[17] The amino groups of PEI on AuNPs exhibit strong interaction with both biomolecules and metal ions and preserve physical and chemical stabilities of conjugates and bioactivity,[17,18] thus resulting in good device performances and stability. Moreover, PEI can conjugate covalently to many particles *via* amide linkages, thus giving stability in aqueous solutions.[16] A majority of label-free type sensors depend on redox species in solutions such as $K_3[Fe(CN)_6]$ and $K_4Fe(CN)_6$ species;[19,20] however, these redox species possibly lead to a decrease in the bioactivity of biomolecules.[21] Many attempts have been made to develop a novel label-free electrochemical sensor based on attaching redox species on the electrode surface to eliminate direct contact with antibodies.[20] Polyoxometalates (POMs), well-known anionic molecular metal–oxygen clusters, have attracted increasing interest in various fields such as catalysis, fuel cells, supercapacitors, biology, and medicine due to their unique chemical, structural, and electronic properties.[22–25] Moreover, POMs, especially phosphomolybdic acid (PMA), have received much attention in the field of electrochemistry because of their potential for reversible multielectron redox reactions, which makes them suitable for the construction of immunosensing platforms, acting as redox signal generators during the testing.[26–30] In addition, fabrication of PMA-modified electrodes is simple by the incubation of electrodes in PMA solution since it strongly adsorbs onto the electrode surfaces.[31,32] In acidic solutions, there are three voltammetric peaks of the six electron surface-confined reduction for PMA-modified glassy carbon and boron-doped diamond electrodes in the potential range of −0.10–0.50 V.[32] The redox process of PMA involves a fast proton-coupled electron transfer reaction.[31,32] Moreover, PMA offers reversible multi-step and multi-electron transfers.[33] Interestingly, PMA can be attached to other kinds of nanomaterials such as poly(3,4-ethylenedioxythiophene) coated AuNPs,[34] poly(diallyldimethylammonium chloride)-reduced graphene oxide (rGO)-modified electrode,[35] and rGO.[36] In such materials, PMA presents good and stable electrochemical responses.[34–36] Furthermore, a polypyrrole@2D $Ti_3C_2T_x$ MXene/PMA nanohybrid can show an extremely low detection limit in an aptasensor.[33] Therefore, PEI-AuNPs and PMA are chosen as electrochemical supports for both immobilization of antibodies and signal amplification. Consequently, the primary goal of this research is to develop a label-free electrochemical immunosensor for sensitive detection of GM2AP in human serum.

In this study, we report a novel label-free immunosensor for highly sensitive detection of a new lung cancer biomarker, GM2AP, based on a PMA/PEI-AuNP-modified screen-printed carbon electrode (SPCE), for the first time. PEI-AuNPs synthesized using PEI as reducing agents were employed as excellent adsorption supports for loading PMA redox probes in a short time. The redox molecules were adsorbed onto the surface of PEI-AuNPs *via* electrostatic interactions, which resulted in a novel PMA/PEI-AuNP-modified SPCE for the fabrication of an electrochemical immunosensor. PEI-AuNPs also have a great capacity for loading antibodies, which have high sensitivity and selectivity for sensing. The results show that the proposed sensor shows excellent sensing performances and offers a simple and rapid alternative way for clinical diagnosis by assaying GM2AP in both human urine and serum.

Experimental

Materials and chemicals

Recombinant human GM2A protein (lot: E32211-8929) and anti-GM2A antibody (lot: GR87284-8) were purchased from Abcam (USA). Phosphomolybdic acid hydrate (PMA, ≥95%) was obtained from Sigma-Aldrich (India). Polyethylenimine (PEI, branched, $M_w \approx 800$) and gold(III) chloride hydrate ($HAuCl_4{\cdot}xH_2O$, 99.999% trace metals basis) were obtained from Sigma-Aldrich (Singapore). Alpha-fetoprotein (AFP, lot: A16042812, 6.9 mg mL^{-1}, >98%) was obtained from Fitzgerald Industries International (USA). Interleukin-15 (IL-15, lot: 2381730, ≥98%) was purchased from Millipore (USA). Glutaraldehyde solution ($C_5H_8O_2$, 50 wt% in H_2O) was purchased from Sigma-Aldrich (Germany). Bovine serum albumin (BSA, lot: D00155527, 98%) was obtained from Calbiochem (USA). Sodium acetate ($CH_3COONa{\cdot}3H_2O$, 99.1%) was purchased from Fisher Scientific (USA). Acetic acid (99.7%) was obtained from RCI Labscan (Thailand). Potassium ferricyanide ($K_3[Fe(CN)_6]$, 99%) was purchased from Merck (Germany). Dopamine hydrochloride (DA, 98%) was obtained from Sigma-Aldrich (Germany). Furthermore, D-(+)-glucose (Glu, ≥99.5%), uric acid (UA, ≥99%), L-ascorbic acid (AA, 99%), phosphate-

buffered saline (PBS) tablets (pH 7.4), potassium hexacyanoferrate(II) trihydrate ($K_4[Fe(CN)_6]\cdot 3H_2O$, 99%), myoglobin (MB, lot: SLBH5660 V, 2.4 mg mL^{-1}, ≥95%), immunoglobulin G (IgG, lot: 082M4772 V, 4.8 mg mL^{-1}, ≥95%), and human serum from human male (AB plasma, USA origin, lot: SLBS6544) were purchased from Sigma-Aldrich (USA). Deionized water (DI) was used throughout these experiments.

Apparatus

Scanning electron microscopy (SEM) images were recorded using a field emission scanning electron microscope (FE-SEM; JSM-6335F, JEOL). Transmission electron microscopy (TEM) was performed using a JEM 2010 (JEOL). Electrochemical experiments including cyclic voltammetry (CV) and differential pulse voltammetry (DPV) were performed using an EmStat3 potentiostat (PalmSens, Netherlands). Electrochemical impedance spectroscopy (EIS) was performed using an Autolab PGStat 20 (Metrohm Autolab B.V, Utrecht, Netherlands). UV-visible (UV-vis) spectra were recorded using an Evolution 201 (Thermo Scientific). Centrifugation was performed using a Digicen 21 (Orto alresa). Electrochemical measurements were performed using a three-electrode electrochemical cell, consisting of a screen-printed carbon-based electrode (SPCE) as a working electrode and platinum wire and a silver/silver chloride (Ag/AgCl, 3 M NaCl) electrode as the auxiliary electrode and reference electrode, respectively. The CV measurements were performed from −0.40 to 0.80 V at a scan rate of 50 mV s^{-1}. The DPV measurements were carried out in the range of −0.40 to 0.80 V at a scan rate of 50 mV s^{-1} at an amplitude of 50 mV and a step potential of 5.0 mV while the EIS measurements were performed at frequencies ranging from 10^{-1} to 10^5 Hz with an alternating current voltage amplitude of 10 mV.

Synthesis of PEI-AuNPs

In this study, PEI-AuNPs, as signal amplifier supports, were synthesized under mild conditions using PEI as the reductant and stabilizer. The PEI-AuNPs were synthesized according to the previous protocol with slight modifications.[17] Briefly, 0.90 mL solution of PEI (1.0 wt%) was quickly injected into 25 mL $HAuCl_4$ aqueous solution (1.40 mM) in a round bottom flask. Then, the reaction mixture was stirred at 800 rpm at room temperature for at least 16 h; immediately the colour changed from yellow to wine-red, indicating the formation of PEI coated AuNPs. The PEI-AuNP sediment was collected after centrifugation at 9000 rpm for 10 min and then was redispersed in DI water, obtaining the maximum absorption peak at 525 nm. Finally, the PEI-AuNP solution was stored at a temperature of 4 °C until use.

Fabrication of an immunosensor and detection of GM2AP

Firstly, an SPCE (3.0 mm diameter) was treated at 400 mbar for 1 min with O_2 plasma. The working area of the SPCE was coated with 5.0 μL PEI-AuNP solution and allowed to dry in air at room temperature. Subsequently, 10 μL of 1.0 mM PMA was adsorbed onto PEI-AuNP-modified SPCE for 1 min at room temperature. The obtained electrode was washed with DI water several times to remove unbound PMA, and then the PMA-PEI-AuNPs were formed *via* electrostatic interactions. Then, 10 μL anti-GM2AP solution was dropped on the PMA/PEI-AuNP-modified electrode for incubation at room temperature for 40 min. After washing with PBS (0.010 M, pH 7.4) to remove the excess anti-GM2AP, the electrode modified with anti-GM2AP was incubated with 10 μL BSA (0.50%w/v) for 30 min at room temperature to block the remaining active sites and non-specific adsorption, followed by washing with PBS buffer several times. Finally, the BSA/anti-GM2AP/PMA/PEI-AuNP modified electrode was then used for the electrochemical detection of GM2AP. The fabrication procedure of the proposed immunosensor is shown in Scheme 1.

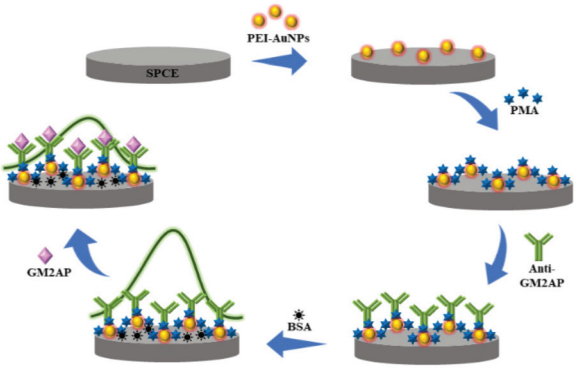

Scheme 1 The immunosensor construction and the electrochemical immunosensing detection of GM2AP.

In our immunosensor, the PMA/PEI-AuNP composite film was fabricated for antibody immobilization and signal amplification. The PEI coating of the AuNPs is particularly attractive because it provides the AuNPs with specific properties such as improved stability against aggregation.[17,25] As shown in Scheme 1, PEI-AuNPs bind with PMA *via* strong electrostatic interactions between the positively surface charged PEI-AuNPs and the highly negatively charged PMA to form a PMA/PEI-AuNP composite film. Anti-GM2AP was immobilized onto the working electrode surface modified with the PMA/PEI-AuNP composite film through electrostatic interaction and hydrogen-bonding.[25]

The GM2AP was detected with DPV measurements in 0.20 M acetate buffer (pH 4.5). The pH value of the electrolyte is optimized (Fig. S1†). The DPV current responses decreased with increasing concentration of GM2AP due to the inhibition effect of insulating protein layers in the proton transfer process from the aqueous phase to govern a proton-coupled electron transfer reaction.

Results and discussion

Characterization of materials and the modified electrodes

Various techniques were performed to investigate the modification of PMA/PEI-AuNPs nanocomposites onto the surface of

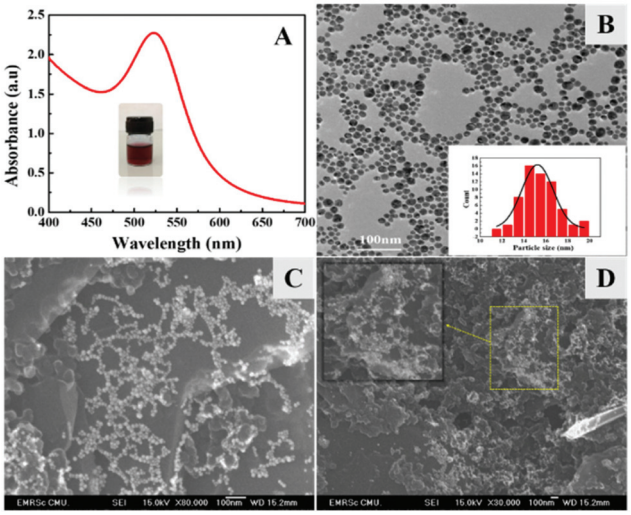

Fig. 1 (A) UV-vis absorption spectrum, (B) TEM image and (C) SEM image of PEI-AuNPs and (D) the SEM image of PMA/PEI-AuNPs synthesized in this study. The absorption spectrum of PEI-AuNPs exhibits a maximum peak at 525 nm.

the working electrode, including SEM, TEM, and UV-vis spectroscopy. The synthesized PEI-AuNPs were characterized by UV-vis absorption spectroscopy as shown in Fig. 1A. The spectrum of AuNPs shows a maximum absorption peak at 525 nm that is ascribed to the SPR band of AuNPs. The shape and size of the spherical AuNPs are investigated by TEM analysis as shown in Fig. 1B. The average particle size of PEI-AuNPs is 15.4 nm in diameter, which provides a high surface area for immobilizing active molecules. Therefore, the results indicate that PEI-AuNPs in this size and shape are successfully synthesized under mild conditions. The morphologies of bare SPCE and PEI-AuNPs-, PMA-, and PMA/PEI-AuNPs-modified SPCEs were characterized by the SEM technique as illustrated in Fig. S2 (in the ESI†). After the PEI-AuNPs were modified onto the electrode surface, homogeneous distribution and narrow size range of PEI-AuNPs are observed (Fig. S2B and S2D†) (the high magnification SEMs of Fig. S2B and S2D† are shown in Fig. 1C and D, respectively), while the unmodified electrode shows no presence of PEI-AuNPs (Fig. S2A†). The results confirm that PEI-AuNPs are successfully modified onto the electrode surface. The uniform distribution of granular PEI-AuNPs could improve the electroactive surface area of the SPCE and provide a large specific surface area to load antibodies onto the electrode as well as offer an absorbable surface for PMA uptake, being able to amplify the analytical current response due to the immunoreaction. To verify the presence of PMA on the electrodes, energy dispersive spectroscopy (EDS) analysis was performed on the electrode surfaces without and with PEI-AuNPs (Fig. S2C and S2D,† respectively). The presence of Mo atoms, as seen in the insets of Fig. S2C and S2D (in the ESI†), indicates that a small amount of PMA has been adsorbed on the surface of both naked and PEI-AuNP-modified SPCEs, respectively.

Electrochemical properties of the modified electrodes

The role of each component in the PMA/PEI-AuNP nanocomposite was studied by the CV and EIS techniques. As shown in Fig. S3A (in the ESI†), the CVs of bare SPCE and PMA-, PEI-AuNPs- and PMA/PEI-AuNP-modified electrodes are studied in PBS (pH 7.4) containing 5.0 mM $[Fe(CN)_6]^{3-/4-}$ at an applied potential range of −0.40 to 0.80 V and a scan rate of 50 mV s^{-1}. The result shows that when compared to bare SPCE, an increase in peak current is observed for the PMA-modified electrode and more for PEI-AuNPs-modified SPCE, thus indicating improved electrode reactivity. Moreover, when PMA is incorporated onto PEI-AuNP-modified SPCE, the observed peak current is highest, suggesting that AuNPs are beneficial for electron transfer at the electrode. It is observed that the formal potential (E°) of the $[Fe(CN)_6]^{3-/4-}$ redox process is not significantly different (*ca.* 0.215–0.220 V) but low peak-to-peak separation (ΔE_P) values of *ca.* 0.120 and 0.150 V are found for PEI-AuNPs- and PMA/PEI-AuNPs-modified SPCEs, respectively. The ΔE_P value is slightly lower for PEI-AuNPs-modified SPCEs, suggesting the best electron transfer kinetics. Although the PEI-AuNPs-modified SPCE reveals the best electron transfer, signal amplification for the construction of the proposed immunosensor requires PMA. Thus, in our development, PMA/PEI-AuNP-modified SPCE is employed. In addition, EIS is also used to characterize a naked SPCE and the electrodes are modified with different nanomaterials like above. As shown in Fig. S3B (in the ESI†), when an SPCE is coated with PMA/PEI-AuNPs, the electrode shows decreased electron-transfer resistance (R_{ct}) of *ca.* 103 Ω compared to a bare SPCE (*ca.* 855 Ω), suggesting that the PMA/PEI-AuNPs nanocomposite with good conductivity can improve the electron transfer rate of the modified electrode. Furthermore, the lowest R_{ct} value of *ca.* 24 Ω is observed for the PEI-AuNP-modified SPCE, resulting in faster electron transfer. This result agrees well with the CV investigation above. From the above studies, the PMA/PEI-AuNP nanocomposite sitting on SPCE is interesting and can be used as an effective electrochemical immunosensor platform due to the excellent redox activity of PMA and the enhanced electron transfer property by the PEI-AuNPs and the biomolecular loading capacity of the PEI-AuNPs.[17]

Adsorption of PMA on electrodes was investigated by monitoring the DPV response of PMA in 0.20 M acetate buffer (pH 4.5) at a scan rate of 50 mV s^{-1} as illustrated in Fig. S4 (in the ESI†). In the potential range of −0.40 to 0.80 V, it was found that there are three peaks corresponding to the two-electron reduction processes. The first reduction peak is highest for the PMA-modified SPCE while the maximum reduction peak is observed for the third peak of the PMA/PEI-AuNP-modified SPCE. Moreover, the multielectron transfer process for PMA on PEI-AuNP-modified SPCE is much higher than that of PMA on SPCE, indicating that PEI-AuNPs are good adsorbents. To study the electrolyte effect on PMA redox responses over the potential range, Fig. S5 (in the ESI†) shows the CVs of PMA in PMA/PEI-AuNP-modified SPCE in three electrolytes,

i.e., 0.10 M sulfuric acid, 0.20 M acetate buffer (pH 4.5) and 0.010 M PBS (pH 7.4). It is clearly shown that the good electrolyte for PMA redox reaction is sulfuric acid solution and the very poor electrolyte is PBS. Well-defined multistep electron transfer responses with four two-electron transfer reduction processes are observed in the sulfuric acid solution because of its proton-coupled electron transfer process. Moreover, the PMA redox reaction in acetate buffer shows only three couple peaks over this potential range. Although sulfuric acid is a good electrolyte for PMA, in order to amplify the immunoreaction during the measurement and preserve the activity of antibodies, we choose 0.20 M acetate buffer (pH 4.5) as the electrolyte for our study throughout the electrochemical measurement. The electrochemical characteristics of the PMA/PEI-AuNP-modified electrode in 0.20 M acetate buffer (pH 4.5) are again investigated by the CV and DPV techniques, as shown in Fig. S6 (in the ESI†). From the CV response, it can be seen that the three reversible redox peaks of the modified electrode are attributed to the redox reaction character of PMA in the PMA/PEI-AuNP nanocomposite-modified SPCE. The three redox peaks located at the potentials 0.338, 0.075, and −0.104 V correspond to three successive two-electron reduction processes I, II, and III, respectively (Fig. S6A†), in which process III reveals the highest current density. In addition, the DPV response is also collected in the same electrolyte. It is found that the three redox peaks at the potentials 0.305, 0.065, and −0.105 V correlate to the three processes I, II, and III, respectively, as shown above in Fig. S6B (in the ESI†). Moreover, process III presents the best current signal which agrees with that from CV. Compared to the CV response, the DPV response has much higher current sensitivity and better resolution in terms of the signal-to-noise ratio. Thus, the DPV technique is used for the development of the immunosensor. Since the peak of process III gives the best electrochemical sensitivity, our immunosensor is demonstrated employing this response for further study of the signal amplification. In order to obtain the reproducibility of the PMA/PEI-AuNP-modified SPCE, the maximum adsorption of PMA is required. Therefore, the optimization of the adsorption period of PMA on the PEI-AuNP-modified SPCE is studied *via* the measurement of the DPV response of process III as depicted in Fig. S7 (in the ESI†). The current reaches a maximized point at which it suggests the highest PMA uptake. The adsorption period is investigated by the incubation of PEI-AuNP-modified SPCE in PMA solution for 10 s to 30 min. It is found that no significant current difference is observed at above 1 min incubation time. The rate of adsorption of PMA is found to be fast from the initial time to 1 min, and then the adsorption goes insignificantly further from 1 to 30 min, thus implying the saturation of PMA molecules adhering to the surface of a PEI-AuNP-modified SPCE. The fast adsorption at the initial stage might result from the large number of surface sites available on the surface of the absorbent, PEI-AuNP-modified SPCE. Interestingly, in order to be aware of the time consumed, the preparation of PEI-AuNP-modified SPCE needs a few minutes, including a step of washing out the excess or unbound PMA molecules. Therefore, the optimum adsorption time of PMA is chosen as 1 min for further experiments.

Study of the fabrication steps and optimization of fabrication conditions

Fig. 2 shows the fabrication process of our immunosensor by employing the prepared PMA/PEI-AuNP-modified SPCE. DPV measurements were performed to monitor the immobilization steps. It is shown that every step causes lowered current responses due to the deposition of insulating molecules (antibodies and BSA) on the electrode, which restrict the proton transfer from the solution during the electron transfer process of PMA on the PMA/PEI-AuNP-modified SPCE. As seen in Fig. 2, a black line represents the DPV response of the bare PMA/PEI-AuNP-modified electrode (*ca.* 39.37). After the electrode is sequentially incubated with 60 μg mL^{-1} anti-GM2AP, 0.50% w/v BSA, and 5.0 ng mL^{-1} GM2AP solutions, the redox peak current decrease as *ca.* 31.34, 29.27, and 23.24 μA, respectively, and the peak position slightly shifts from −0.100 V to −0.110 V. This results from the biologically active substances, thus hindering the efficiency of proton transfer from the aqueous phase to maintain the charge neutrality of PMA on the electrode surface and lowering the ability of the proton-coupled electron transfer process of PMA. Clearly, the assembly of these biomolecules on the electrode surface to form an immunosensor is successful. Additionally, adding each biomolecular layer would form an ion-barrier, causing the reduction of the current response.[37,38] Moreover, the immobilization of anti-GM2AP antibodies with and without a cross-linking process by employing a 2.5 wt% glutaraldehyde solution is examined as illustrated in Fig. S8 (in the ESI†). It is found that the responses from both cases have an insignificant difference, indicating the same amount of electrode-confined antibodies, which would offer similar sensitivity and device performances in terms of target-capture capacity. This implies that both sensors would have no significant difference in the current response due to the incubation of the GM2AP solution at the same concentrations. As a result, it is plausible that the

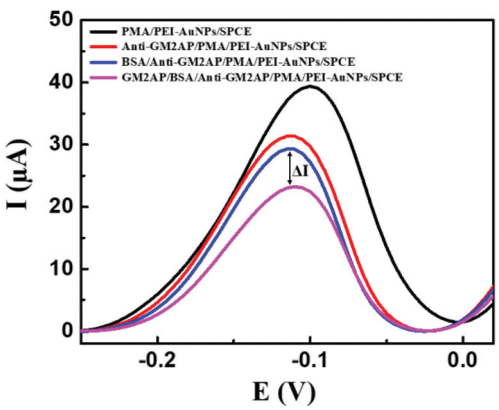

Fig. 2 DPV current responses of SPCE measured in 0.2 M acetate buffer (pH 4.5) for each step of the modification.

ability of the PMA/PEI-AuNP nanocomposite on SPCE in the immobilization of antibodies is sufficient. Therefore, for the construction of our immunosensor, we prepared the immunosensor without the crosslinking process owing to the time-consuming step. Our immunosensor not only reduces this step of fabrication but also reduces the number of chemicals used.

The amount of immobilized antibodies (anti-GM2AP) is another main parameter affecting device performances, especially its sensitivity and selectivity. It is expected that according to Fig. 2, the immobilization of anti-GM2AP antibodies on the surface of PMA/PEI-AuNP-modified SPCE causes the reduced response of PMA. Consequently, the surface saturation of the antibodies results in no further significant change in the response or a constant response was obtained. This saturation indicates a maximum loaded amount of the antibodies on the electrode surface, in turn giving the best device. To obtain this highest protein loading, at the incubation period of 40 min, the effect of the concentration of the anti-GM2AP antibodies is investigated and the concentration is varied from 20 to 100 μg mL^{-1}. It can be seen in Fig. 3A that the current starts with a constant value at a concentration of 60 μg mL^{-1} of anti-GM2AP. This is caused by the saturation of loaded anti-GM2AP antibodies. Thus, 60 μg mL^{-1} is used for investigating the optimal incubation time for anti-GM2AP immobilization. Additionally, a too short period giving antibody unsaturation would affect the stabilities of the immunosensor as the surface saturation or maximum loading of the antibodies requires enough time for electrostatic binding. In terms of saving time for the fabrication of the proposed immunosensor, the immobilization of anti-GM2AP antibodies on the PMA/PEI-AuNP-modified SPCE incubated in the anti-GM2AP solution from 10 to 60 min is studied as shown in Fig. 3B. It is found that for an incubation time of 40 min, the current remains constant, suggesting the saturation of anti-GM2AP antibodies. This period of time is selected for the next optimization and as the fabrication condition. For the measurement of GM2AP concentration, the immunoreaction needs sufficient time during the incubation of antibody-bound electrode surface with the antigen solution. The incubation time for the immunoreaction between the antigen (GM2AP) and immobilized antibody (anti-GM2AP) was optimized from 10 to 60 min. Fig. 3C shows that the peak current rapidly decreases with the increment in incubation time and then tends to level off after an incubation of 40 min, indicating the complete formation of immunocomplexes or complete immunoreaction. Therefore, the period of time of 40 min is the optimized incubation time in this study.

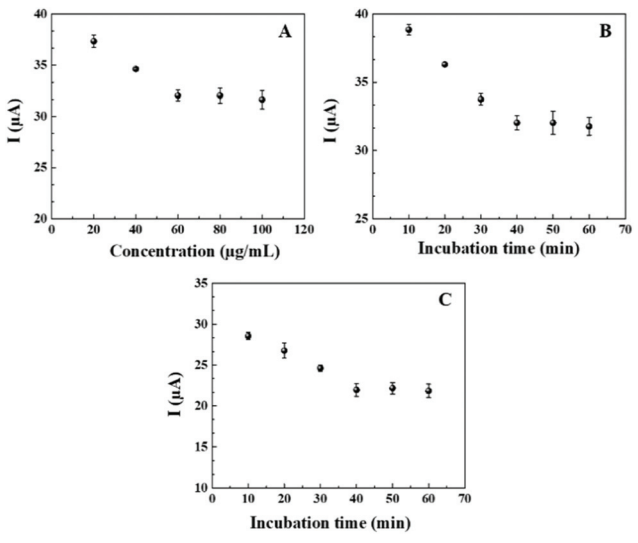

Fig. 3 Optimizations of (A) antibody concentration and (B) incubation time for the immobilization of antibody and (C) incubation time for the immunoreaction. All experiments were performed using the DPV technique in 0.20 M acetate buffer (pH 4.5) at a scan rate of 50 mV s^{-1}.

Performance of the immunosensor

After the construction of the GM2AP immunosensor under the optimized conditions, the performance of the immunosensor was tested by the detection of GM2AP at different concentrations. The peak current decreases with the increasing concentration of GM2AP as shown in Fig. 4A. The decreasing electrochemical current response indicates the biologically active substance, namely antigen (GM2AP), bound on the immunosensing electrode, which can hinder the efficiency of proton transfer from the aqueous phase. A good linear relationship is obtained between the DPV response and the logarithm value of GM2AP concentration in the range of 0.005 to 25 and 25 to 400 ng mL^{-1} with correlation coefficients of 0.9859 and 0.9955, respectively, as shown in Fig. 4B. This results from the different blockage mechanisms of proton (H^+ ion) transfer to such immunosensing surfaces. The limit of detection (LOD) is experimentally obtained (3SD/slope) and found to be 0.51 pg mL^{-1}. In addition, the GM2AP level in healthy human urine and serum are significantly less than 1.46 and 0.92 ng mL^{-1}, respectively.[7] The LOD of the biosensor is approximately 2863 and 1804 fold lower than the clinically relevant levels in the human urine and serum of patients with lung cancer, respectively.[7] Therefore, the proposed immunosensor could be used for the testing and screening of lung cancer *via* the determination of GM2AP in human fluids with

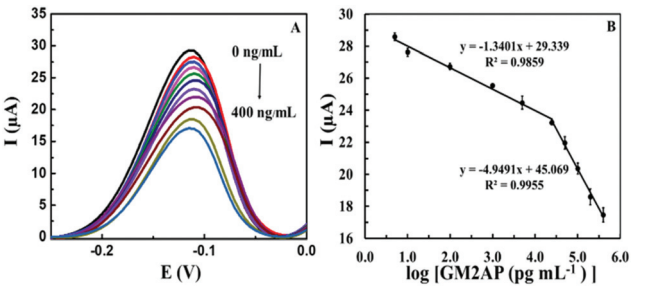

Fig. 4 (A) DPV responses after incubation with different GM2AP concentrations and (B) the corresponding calibration curve of the immunosensor, n = 3. The measurements were performed in contact with 0.20 M acetate buffer (pH 4.5) at a scan rate of 50 mV s^{-1}.

the features of low LOD, high detection accuracy, and sensitivity.

The selectivity of the immunoassay was evaluated by incubating with 5.0 ng mL^{-1} GM2AP solution without and with different interfering substances (*e.g.*, IgG, AFP, IL-15, MB, DA, Glu, AA, UA, and a mixture of all) at a concentration of 500 ng mL^{-1}. The solutions of each individual interferent and a mixture of all interferents at the same concentration were also employed. Fig. 5 shows the measured currents after the surface of the anti-GM2AP/PMA/PEI-AuNP-modified SPCEs are soaked with all the above different solutions including a PBS solution as a blank (*ca.* 29 μA). With the absence of GM2AP in the solutions, no significant differences (less than 3.4% from that of blank) in the current responses are observed for the blank, all individual interferent solutions, and an interferent mixture, indicating that non-specific adsorption is low and does not influence the electrochemical reaction of the PMA. With the existence and co-existence of GM2AP in the solutions, the current response significantly changes to a lower value (*ca.* 24 μA) due to the immunoreaction, indicating the good selectivity in detecting GM2AP. The current differences among the solutions with the presence of GM2AP are less than 4.2% as compared to that of the GM2AP solution with no interferents, thus confirming no effect of non-specific adsorption. In addition, the reproducibility of the developed GM2AP immunosensor was investigated. Fifteen sensors were constructed using the same conditions and employed to detect 5.0 ng mL^{-1} GM2AP. Fig. S9 (in the ESI†) shows the currents after the incubation of the immunosensors with the GM2AP solution. The relative standard deviation (RSD) of the measurement for the fifteen sensors is of *ca.* 2.0%, indicating that the reproducibility of the proposed immunosensor is greatly acceptable. Furthermore, to test the stability of the proposed immunosensor, the storage lifetime was investigated. The prepared sensors after the immobilization of the anti-GM2AP capture antibody were stored at a temperature of 4 °C for future use. As shown in Fig. S10 (in the ESI†), the current response of the prepared immunosensor is decreased by 1.6% after a seven-day storage. The current response is decreased to *ca.* 91% of the initial response with a 42-day storage, implying that our proposed sensor has high stability. The good stability of the immunosensor may be attributed to the sufficient electrostatic interaction of anti-GM2AP and/or PMA with PEI-AuNPs and the biocompatibility of PEI-AuNPs[17] that would preserve the bio-reactivity of anti-GM2AP. The specificity, reproducibility, and stability of the proposed biosensor are satisfactory. Therefore, the proposed immunosensor can be demonstrated as an alternative tool for the sensitive determination of GM2AP at the critical levels. Moreover, there is no report about the electrochemical determination of GM2AP. In our study, for the first time, the immunosensor for the quantitative detection of GM2AP employing PMA and PEI-AuNPs is carried out. Previously, PMA was employed in the construction of DNA and aptamer biosensors as listed in Table S1 (in the ESI†). Interestingly, our human GM2AP immunosensor can be operated with a broader sensitivity limit as compared to that of the standard method, sandwich enzyme-linked immunosorbent assay (ELISA).[7]

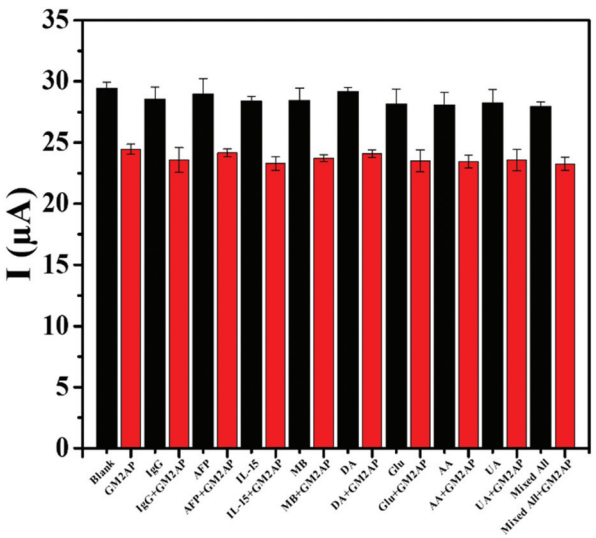

Fig. 5 Interference study of the developed immunosensor for the detection of GM2AP (5.0 ng mL^{-1}) and GM2AP with interferences (500 ng mL^{-1}) in 0.20 M acetate buffer (pH 4.5).

Application in the analysis of GM2AP in human serum and urine samples

In order to evaluate the reliability of our strategy, the proposed GM2AP immunosensor was applied to detect GM2AP in human serum and urine samples that were spiked with different GM2AP concentrations. The spiked amounts of GM2AP in the serum and urine samples, which are employed as blanks, are 1.0, 2.5, 5.0, 10, and 20 ng mL^{-1}, and the recoveries of the five GM2AP concentrations in both samples were evaluated. As shown in Table 1, the ranges of the recoveries of GM2AP in the serum and urine samples are 98.88–106.53% and 93.88–107.91%, respectively. The relative standard deviations (RSD) of the analysis for the human serum and urine

Table 1 Recovery test of GM2AP in human serum and urine samples obtained by the proposed immunosensor. These experiments were performed in triplicate

Biological samples	GM2AP spiked (ng mL^{-1})	GM2AP measured (ng mL^{-1})	% Average recovery	RSD (%)
Human serum (n = 3)	1	1.02 ± 0.07	102.46	6.83
	2.5	2.47 ± 0.14	98.88	5.66
	5	5.28 ± 0.17	105.64	3.22
	10	10.65 ± 0.45	106.53	4.22
	20	20.54 ± 0.46	102.71	2.24
Urine (n = 3)	1	1.01 ± 0.04	100.62	3.98
	2.5	2.35 ± 0.11	93.88	4.62
	5	5.23 ± 0.20	107.08	3.73
	10	10.55 ± 0.62	107.91	5.70
	20	20.86 ± 1.02	104.30	4.89

are 2.24–6.83% and 3.73–5.70%, respectively, verifying a good precision of the proposed detection strategy. Hence, it clearly shows that our proposed PMA/PEI-AuNPs-based immunosensor has the potential to detect GM2AP in real human serum and urine samples and evaluate patients with lung cancer.

Conclusions

A novel and simple PMA/PEI-AuNPs-modified SPCE used as a label-free immunosensing platform is successfully developed for highly sensitive GM2AP detection in human urine and serum for the first time. The modified SPCE exhibits good conductivity and well-defined redox peaks of adsorbed PMA, which is a signal amplifier due to the blockage of its electrochemical reaction. A high adsorption amount of PMA on the electrode with the presence of PEI-AuNPs is observed because of the strong electrostatic interaction between PMA and the PEI-AuNP surface. The proposed GM2AP immunosensor displays two wide linear dynamic ranges and its LOD is significantly lower than the cut-off levels. In addition, this label-free immunosensor provides high selectivity, good reproducibility, and high stability over six weeks (*ca*. 91% remaining response), which shows its potential application in the detection of the new lung cancer biomarker, GM2AP, for clinical diagnosis and in the development of clinical detection of other tumor markers.

Live subject statement

All experiments were performed in accordance with the International Ethical Guidelines for Biomedical Research Involving Human Subjects of the World Health Organization and approved by the Chiang Mai University Ethical Committee (CMUREC 61/039). Informed consent was obtained from the human participants of this study.

Author contributions

Kulrisa Kuntamung: investigation, writing – original draft. Padchanee Sangthong: writing – review & editing. Jaroon Jakmunee: writing – review & editing. Kontad Ounnunkad: conceptualization, methodology, validation, resources, writing – original draft, writing – review & editing, visualization, supervision, project administration, funding acquisition.

Conflicts of interest

There are no conflicts to declare.

Acknowledgements

This work was supported by the Chiang Mai University (CMU) and CMU Mid-Career Research Fellowship program. K. K. would like to thank an award of the Science Achievement Scholarship of Thailand (SAST). The authors gratefully acknowledge the Graduate School (CMU), Research Center on Chemistry for the Development of Health Promoting Products from the Northern Resources, the Center of Excellence for Innovation in Chemistry (PERCH-CIC), the Center of Excellence in Materials Science and Technology, and the Department of Chemistry, Faculty of Science, CMU. The authors acknowledge the financial support from the Program Management Unit for Human Resources & Institutional Development, Research and Invitation, NXPO [Frontier Global Partnership for Strengthening Cutting-edge Technology and Innovations in Materials Science].

References

1 Z. Altintas and I. Tothill, *Sens. Actuators, B*, 2013, **188**, 988–998.
2 T. N. Zamay, G. S. Zamay, O. S. Kolovskaya, R. A. Zukov, M. M. Petrova, A. Gargaun, M. V. Berezovski and A. S. Kichkailo, *Cancers*, 2017, **9**, 155.
3 A. Roointan, T. A. Mir, S. I. Wani, R. Mati ur, K. K. Hussain, B. Ahmed, S. Abrahim, A. Savardashtaki, G. Gandomani, M. Gandomani, R. Chinnappan and M. H. Akhtar, *J. Pharm. Biomed. Anal.*, 2019, **164**, 93–103.
4 T. Walser, X. Cui, J. Yanagawa, J. M. Lee, E. Heinrich, G. Lee, S. Sharma and S. M. Dubinett, *Proc. Am. Thorac. Soc.*, 2008, **5**, 811–815.
5 M. Kanwal, X.-J. Ding and Y. Cao, *Oncol. Lett.*, 2017, **13**, 535–542.
6 M. Sharifi, M. R. Avadi, F. Attar, F. Dashtestani, H. Ghorchian, S. M. Rezayat, A. A. Saboury and M. Falahati, *Biosens. Bioelectron.*, 2019, **126**, 773–784.
7 L. Potprommanee, H. T. Ma, L. Shank, Y. H. Juan, W. Y. Liao, S. T. Chen and C.-J. Yu, *J. Thorac. Oncol.*, 2015, **10**, 102–109.
8 L. Potprommanee, H. T. Ma, C. H. Chen, P. Aobchey, K. Boonyapranai, B. Chewaskulyong, P. Sangthong, L. Shank and S. T. Chen, *J. Proteomics Bioinf.*, 2013, **6**, 264–270.
9 H. Radecka and J. Radecki, *J. Mex. Chem. Soc.*, 2015, **59**, 269–275.
10 Z. Huang, Z. Jiang, C. Zhao, W. Han, L. Lin, A. Liu, S. Weng and X. Lin, *Int. J. Nanomed.*, 2017, **12**, 3049–3058.
11 Q. Yan, Y. Yang, Z. Tan, Q. Liu, H. Liu, P. Wang, L. Chen, D. Zhang, Y. Li and Y. Dong, *Biosens. Bioelectron.*, 2018, **103**, 151–157.
12 L. Liu, Y. Li, L. Tian, T. Guo, W. Cao and Q. Wei, *Sens. Actuators, B*, 2015, **211**, 170–176.
13 Y. Fan, S. Shi, J. Ma and Y. Guo, *Biosens. Bioelectron.*, 2019, **135**, 1–7.
14 Y. Gao, J. Xu, L. Lu, X. Zhu, W. Wang, T. Yang, K. Zhang and Y. Yu, *RSC Adv.*, 2015, **5**, 86910–86918.
15 B. Zhang, Y. Lu, C. Yang, Q. Guo and G. Nie, *Biosens. Bioelectron.*, 2019, **134**, 42–48.

16 C. Yang, Q. Guo, Y. Lu, B. Zhang and G. Nie, *Sens. Actuators, B*, 2020, **303**, 127246.
17 T. Putnin, A. Ngamaroonchote, N. Wiriyakun, K. Ounnunkad and R. Laocharoensuk, *Microchim. Acta*, 2019, **186**, 305.
18 W. J. Song, J. Z. Du, T. M. Sun, P. Z. Zhang and J. Wang, *Small*, 2010, **6**, 239–246.
19 H. Wang, H. Li, Y. Zhang, Q. Wei, H. Ma, D. Wu, Y. Li, Y. Zhang and B. Du, *Biosens. Bioelectron.*, 2014, **53**, 305–309.
20 Y. S. Gao, X. F. Zhu, J. K. Xu, L. M. Lu, W. M. Wang, T. T. Yang, H. K. Xing and Y. F. Yu, *Anal. Biochem.*, 2016, **500**, 80–87.
21 Y. Shen, G. Shen and Y. Zhang, *Anal. Methods*, 2018, **10**, 1612–1617.
22 G. Shah, J. M. Zhao, B. H. Lou, W. Zhang, A. Rehman and G. B. Xu, *Chin. J. Anal. Chem.*, 2017, **45**, E1709–E1712.
23 Z. Bai, C. Zhou, H. Xu, G. Wang, H. Pang and H. Ma, *Sens. Actuators, B*, 2017, **243**, 361–371.
24 J. Chen, P. He, H. Bai, H. Lei, K. Liu, F. Dong and X. Zhang, *J. Electroanal. Chem.*, 2017, **784**, 41–46.
25 D. D. Zhang, Z. Y. Guo, P. F. Guo, X. Hu, X. W. Chen and J. H. Wang, *ACS Appl. Mater. Interfaces*, 2018, **10**, 21876–21882.
26 Z. Wang, Q. Han, J. Xia, L. Xia, S. Bi, G. Shi, F. Zhang, Y. Xia, Y. Li and L. Xia, *J. Electroanal. Chem.*, 2014, **726**, 107–111.
27 T. Wei, Y. Chen, W. Tu, Y. Lan and Z. Dai, *Chem. Commun.*, 2014, **50**, 9357–9360.
28 Y. Ding, B. Du, X. Zhao, J. Y. Zhu and D. Liu, *Bioresour. Technol.*, 2017, **228**, 279–289.
29 S. Zhang, P. He, W. Lei and G. Zhang, *J. Electroanal. Chem.*, 2014, **724**, 29–35.
30 J. Y. Xu, X. Y. Cao, J. F. Xia, S. D. Gong, Z. H. Wang and L. Lu, *Anal. Chim. Acta*, 2016, **934**, 44–51.
31 M. Robinson, K. Ounnunkad, J. Zhang, D. Gavaghan and A. Bond, *ChemElectroChem*, 2018, **5**, 3771–3785.
32 M. Robinson, K. Ounnunkad, J. Zhang, D. Gavaghan and A. Bond, *ChemElectroChem*, 2019, **6**, 5499–5510.
33 S. Zhou, C. Gu, Z. Lib, L. Yang, L. He, M. Wang, X. Huang, N. Zhou and Z. Zhang, *Appl. Surf. Sci.*, 2019, **498**, 143889.
34 S. S. Hassan, Y. Liu, Sirajuddin, A. R. Solangi, A. M. Bond and J. Zhang, *Anal. Chim. Acta*, 2013, **803**, 41–46.
35 L. Ding, Y. Liu, S. X. Guo, J. Zhai, A. M. Bond and J. Zhang, *J. Electroanal. Chem.*, 2014, **727**, 69–77.
36 K. J. Chen, S. Liu, W. Feng, G. Zhang and F. Yang, *Phys. Chem. Chem. Phys.*, 2013, **15**, 5664–5669.
37 K. Kurzatkowska, A. Sirko, W. Zagorski-Ostoja, W. Dehaen, H. Radecka and J. Radecki, *Anal. Chem.*, 2015, **87**, 9702–9709.
38 K. Malecka, A. Stachyra, A. Gora-Sochacka, A. Sirko, W. Zagorski-Ostoja, W. Dehaen, H. Radecka and J. Radecki, *Biosens. Bioelectron.*, 2015, **65**, 427–434.